

# We are IntechOpen, the world's leading publisher of Open Access books Built by scientists, for scientists

6,900

Open access books available

185,000

International authors and editors

200M

Downloads

Our authors are among the

154

Countries delivered to

TOP 1%

most cited scientists

12.2%

Contributors from top 500 universities



WEB OF SCIENCE™

Selection of our books indexed in the Book Citation Index  
in Web of Science™ Core Collection (BKCI)

Interested in publishing with us?  
Contact [book.department@intechopen.com](mailto:book.department@intechopen.com)

Numbers displayed above are based on latest data collected.  
For more information visit [www.intechopen.com](http://www.intechopen.com)



# Repairing Nanoimprint Mold Defects by Focused-Ion-Beam Etching and Deposition

Makoto Okada and Shinji Matsui  
*University of Hyogo  
 Japan*

## 1. Introduction

Nanoimprint lithography (NIL) has been attracting attention from many industries because of its potential use in producing various nanostructure applications through a simple, low-cost, and high-throughput process. There are three primary types of NIL: thermal (T-NIL), UV-NIL, and room-temperature (RT-NIL). T-NIL has a heating and cooling process because thermoset or thermoplastic resins are usually used as T-NIL resins. When a thermoset resin is used, the mold is pressed on a substrate coated with the resin at room-temperature. During pressing, the mold and substrate are heated to harden the thermoset resin, and after cooling, the mold is separated from the substrate. It is slightly different with thermoplastic resin: in this case, the mold is pressed on a substrate coated with the resin at the resin's glass-transition temperature ( $T_g$ ). The mold and substrate temperatures are then decreased and the mold is removed from the substrate. Si,  $\text{SiO}_2/\text{Si}$ , and Ni molds are usually used as T-NIL molds. UV-NIL is a room-temperature process because UV-curable resins are used as UV-NIL resins. The UV-NIL mold is pressed on the substrate coated with UV-curable resin and then the substrate is irradiated with 365-nm UV through the mold. After this irradiation, the mold is separated from the substrate. This means that UV transmissive material must be used as UV-NIL mold material. Generally, a quartz mold is used as a hard mold, and a polydimethylsiloxane (PDMS) mold is used as a soft mold. RT-NIL can be performed without heating, cooling, or UV irradiation. In this process, the sol-gel materials, such as hydrogen silsesquioxane (HSQ), spin-on-glass (SOG), and sol-gel indium tin oxide (ITO), are used as RT-NIL resins. This process requires high pressure, so Si or  $\text{SiO}_2/\text{Si}$  molds are usually used.

What type of mold to use is one of the most important factors in nanoimprint lithography because the mold must come into direct contact with the replication material and the imprinted pattern resolution depends on the mold pattern resolution. The pattern is therefore typically fabricated by electron beam (EB) lithography to obtain a high resolution pattern, thus necessitating a mold repair process with high resolution. In photolithography mask repair, focused ion beam (FIB) etching is used to remove Cr opaque defects, and FIB chemical vapour deposition (CVD), using hydrocarbon precursor gas, is used to repair clear defects. Two types of defect occur in NIL molds –protrusion and hollow defects– which correspond to the opaque and clear defects in photomasks. However, unlike photomask patterns, the NIL relief-structure patterns are formed on a substrate surface. Therefore, we

must perform FIB etching and CVD directly on the substrate material to repair protrusion and hollow defects, respectively. From an economic viewpoint it is best to use existing technology, so we applied FIB etching and CVD to repair the NIL molds and then examined the resulting repair resolution.

2. Thermal nanoimprint mold repair using FIB technique

Watanabe et al. previously reported on SiO<sub>2</sub>/Si mold repair for thermal NIL using FIB etching and CVD. We first fabricated an SiO<sub>2</sub>/Si mold with protrusion and hollow defects by EB lithography and reactive ion etching (RIE). The scanning electron microscopy (SEM) images of the fabricated SiO<sub>2</sub>/Si mold shown in Fig. 1 depict both the (a) protrusion and (b) hollow defects. The width and length of the protrusion defect were 210 and 130 nm, respectively, and the width of the hollow defect was 250 nm.

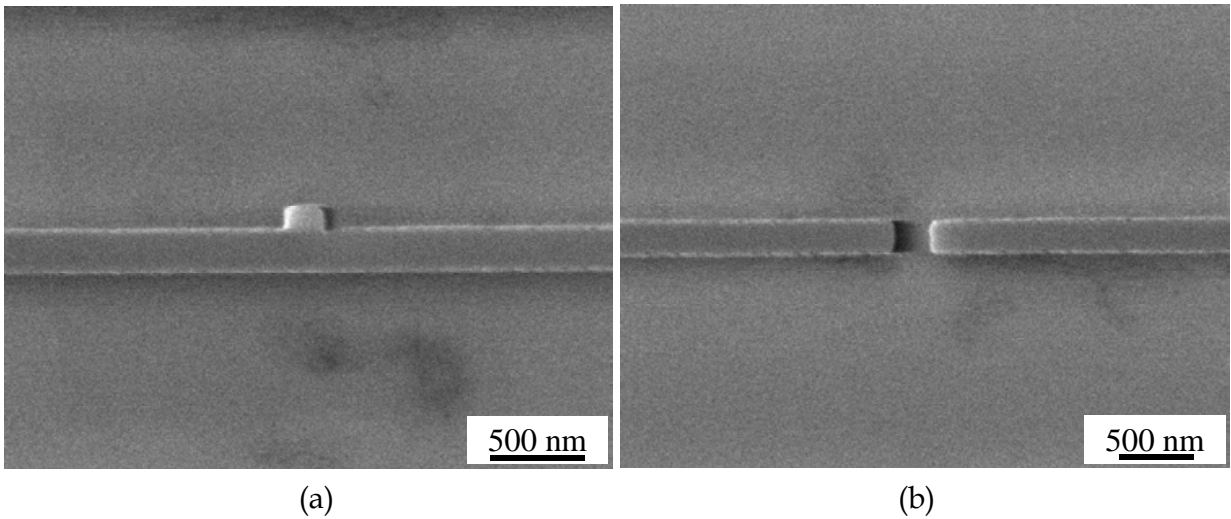


Fig. 1. SEM images of fabricated SiO<sub>2</sub>/Si mold with (a) protrusion and (b) hollow defects.

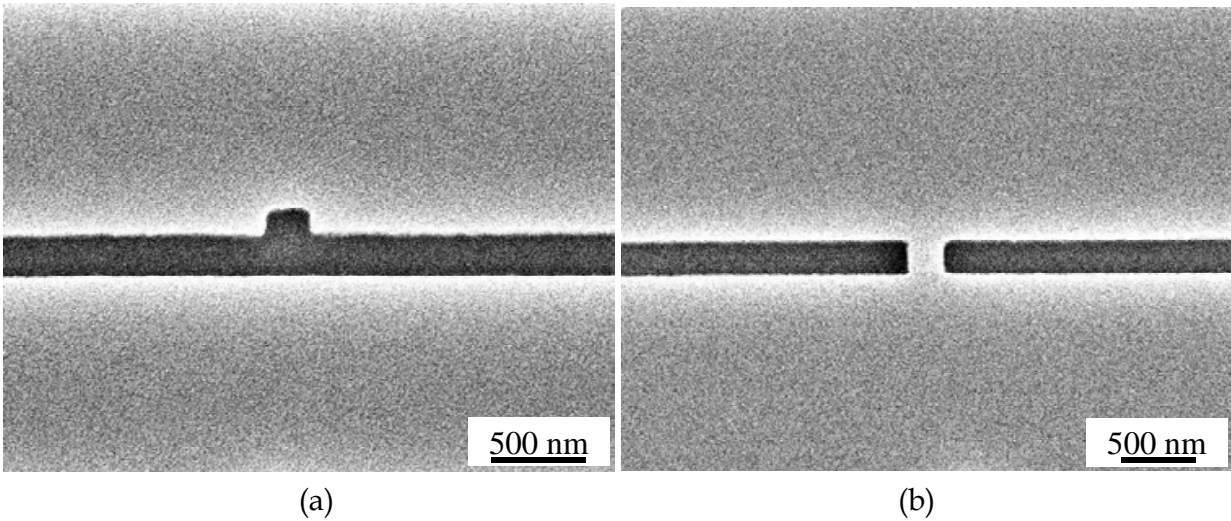


Fig. 2. SEM images of imprinted (a) protrusion- and (b) hollow-defective lines on NEB-22.

We performed thermal nanoimprinting on NEB-22 (Sumitomo Chemical Co.) using this mold. The mold and resin were heated at 150 °C. Imprinting pressure and time were 10 MPa and 1min, respectively. The protrusion and hollow defects were clearly imprinted on the resin. We repaired these defects by FIB etching and CVD.

Figure 3(a) and (b) shows the schematic of the repair process for the protrusion and hollow defects, respectively, on the mold. We used SMI2050MS2 (SII NanoTechnology Inc.) as a FIB system. The ion source, acceleration voltage, and beam current were gallium, 30 kV, and 1 pA, respectively. The protrusion defect was removed by FIB etching. When we repaired the hollow defect, we performed FIB-CVD using phenanthrene ( $C_{14}H_{10}$ ) as a source gas to fill in the hollow defect. Using the phenanthrene caused a diamond-like carbon (DLC) to be deposited, which upon examination we found to contain gallium. Gallium contained in DLC deposited by FIB-CVD can be evaporated by annealing at over 500 °C, but this evaporation does not occur in general thermal nanoimprinting because in such processes the temperature is usually from 100 to 200 °C. Figure 4(a) and (b) shows the SEM images of the repaired  $SiO_2/Si$  mold with protrusion and hollow defects, respectively. The protrusion defect was removed by FIB etching and the hollow defect was filled in by FIB-CVD. The etching and deposition times in this case were about 1 min and 30 sec, respectively. We then performed thermal nanoimprinting using the repaired mold on NEB-22, as shown in Fig. 5(a) and (b). The repaired lines were clearly imprinted on NEB-22. These results indicate that we can repair the protrusion and hollow defects on the thermal nanoimprint mold by FIB etching and CVD.

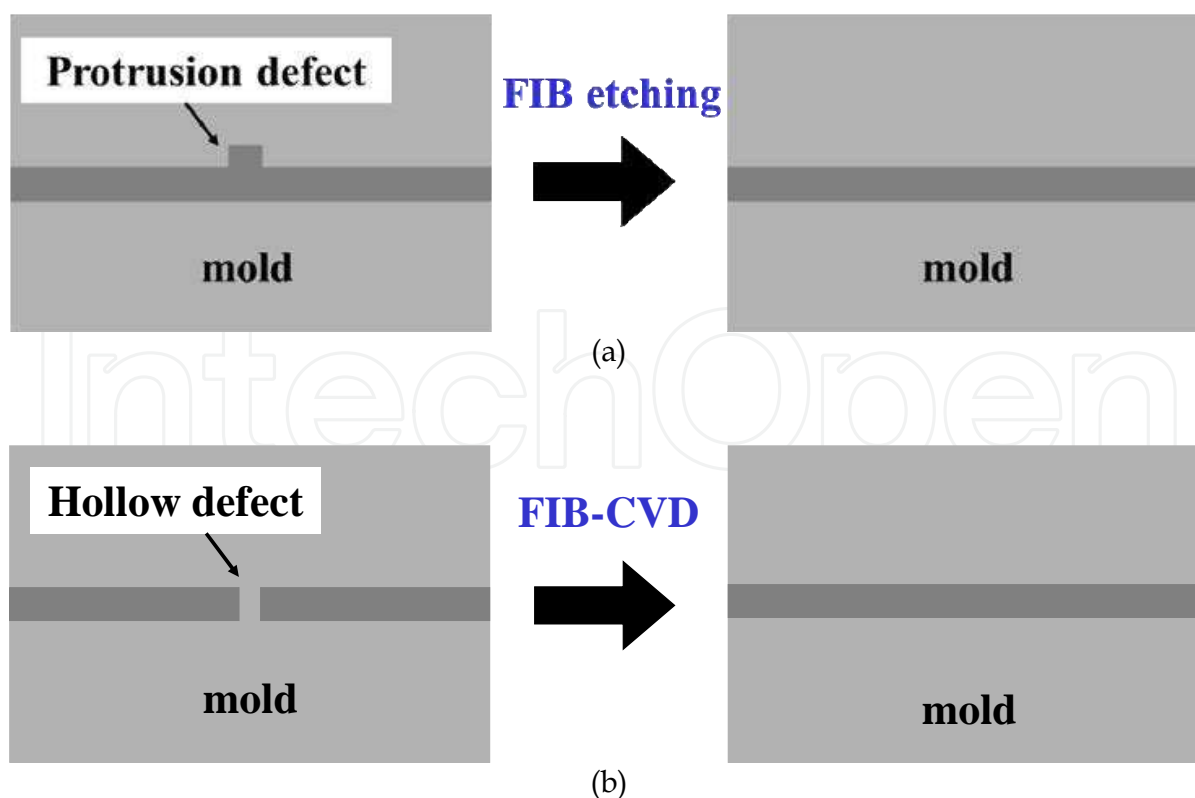


Fig. 3. Schematic of repair process of (a) protrusion and (b) hollow defects on mold.



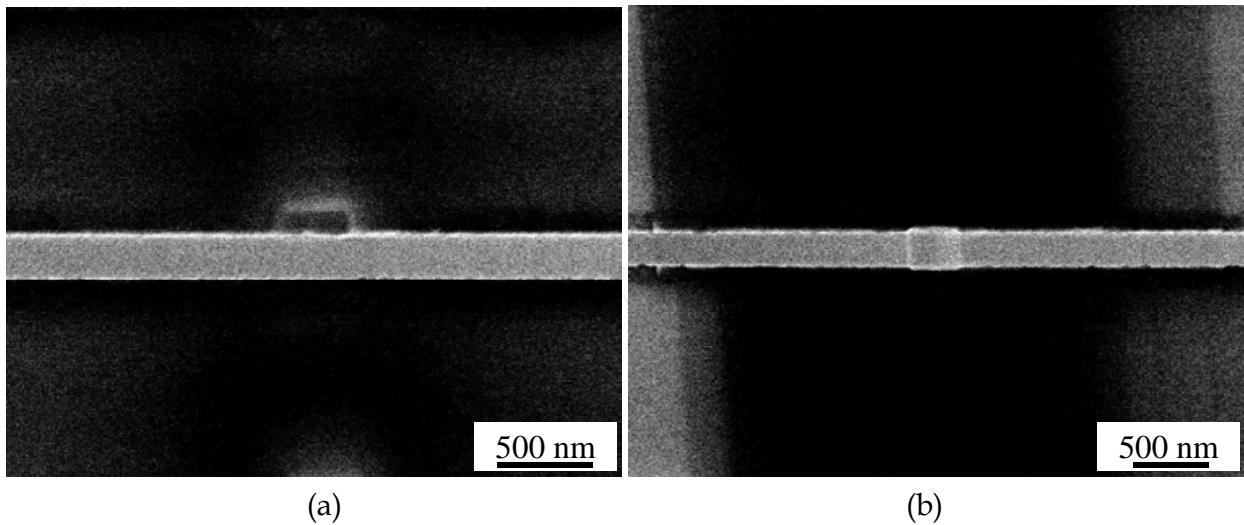


Fig. 4. SEM images of repaired SiO<sub>2</sub>/Si mold with (a) protrusion and (b) hollow defect.

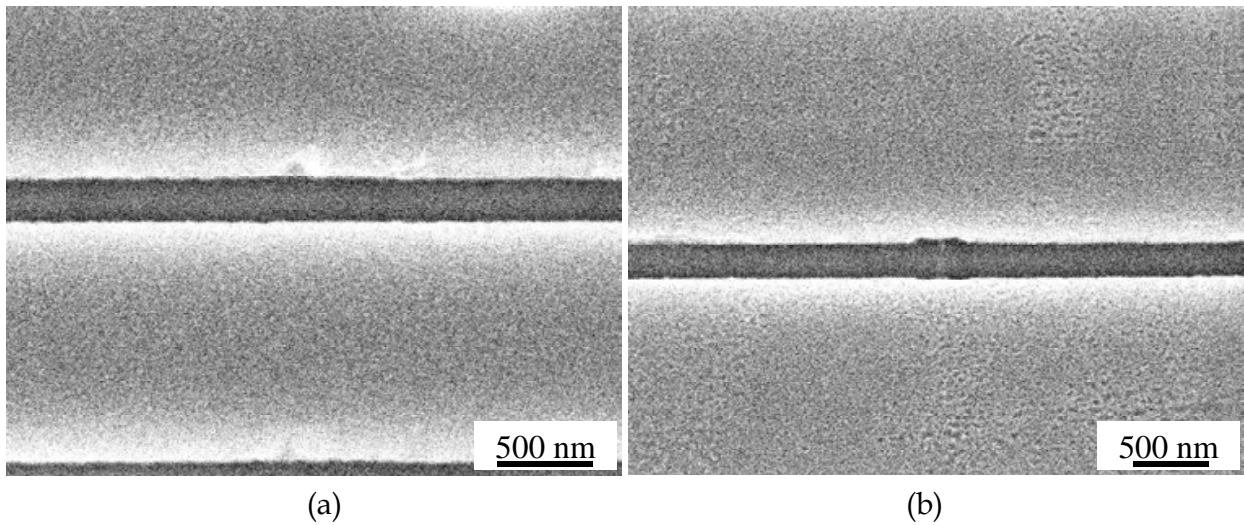


Fig. 5. SEM images of lines imprinted by T-NIL using repaired (a) protrusion- and (b) hollow-defective SiO<sub>2</sub>/Si mold.

3. Repair of UV nanoimprint mold by using FIB etching and CVD

3.1 Characteristics of SiOx material deposited by FIB-CVD using tetraethoxysilane as source gas

In photomask repair and thermal NIL mold repair, the material deposited by FIB-CVD is DLC, which is not clear. In UV-NIL, UV-curable resin is irradiated by UV through the UV-NIL mold. Therefore, the material deposited by FIB-CVD must be transparent, meaning we cannot use DLC as the deposited material. However, we are able to deposit a SiOx material, which is transparent, by FIB-CVD using tetraethoxysilane [Si(OC<sub>2</sub>H<sub>5</sub>)<sub>4</sub>] as a source gas. To examine whether the SiOx-deposited material has sufficient transmittance and hardness to withstand UV-NIL, we measured the atomic composition, transmittance, and hardness of SiOx film fabricated by FIB-CVD using tetraethoxysilane.

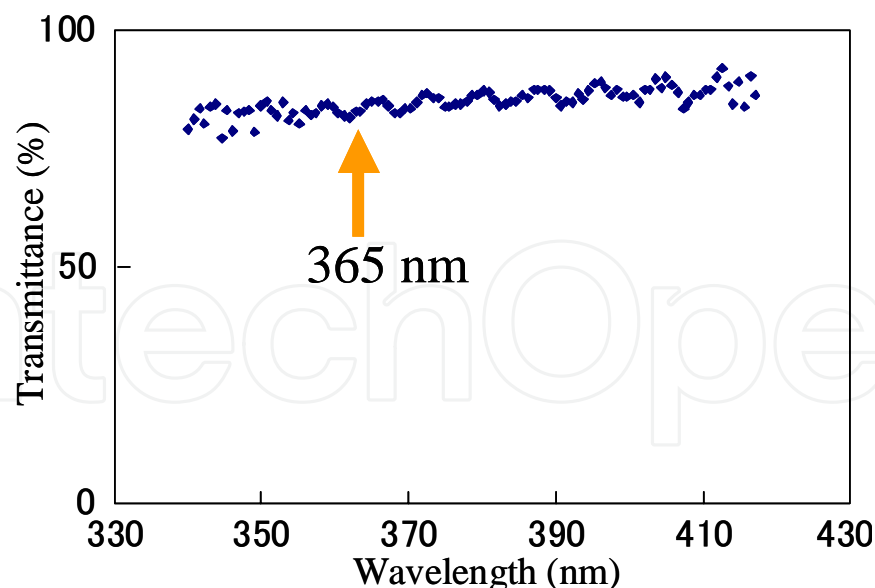


Fig. 6. Transmittance of SiOx film fabricated by FIB-CVD using tetraethoxysilane.

The atomic composition of the SiOx film measured by scanning electron microscopy-energy dispersive X-ray analysis (SEM-EDX) was 13% Si, 58% O, 9% C, and 20% Ga. A small amount of carbon is included in the SiOx film because tetraethoxysilane is composed of Si, O, H, and C. Ga is incorporated into SiOx film because Ga ion implantation is induced by the Ga ion beam used in FIB-CVD. We measured the transmittance of the  $720 \times 720 \mu\text{m}^2$ ,  $1 \mu\text{m}$  thick SiOx film using a monochromator (Hamamatsu Photonics: PMA-11) with a Xenon lamp. Figure 6 shows the results of measuring the SiOx film's transmittance. 365-nm UV is typically used in UV-NIL. The transmittance of the SiOx film was 83 % at 365 nm. This result demonstrated that the SiOx material deposited by FIB-CVD has a sufficient transmittance to carry out UV-NIL. Next, we measured the hardness of the SiOx film with a nanoindenter (Elionix: ENT-1100a). The hardness of the  $150 \times 150 \mu\text{m}^2$ ,  $1 \mu\text{m}$  thick SiOx film was 5 GPa. This result shows that the deposited SiOx material has a sufficient hardness because UV-NIL is usually performed at pressures below 1 MPa. These results clearly demonstrate that SiOx material deposited by FIB-CVD using tetraethoxysilane can be used as the repair material for a UV-NIL mold.

### 3.2 Necessity of antistatic treatment

When FIB is used to repair defective photomasks, the photomasks do not develop a charge because Cr metal patterns are formed on the quartz substrate. On the other hand, UV-NIL molds do develop a charge because the patterns are formed on the surface of the quartz substrate. It is therefore necessary to prevent electrical charge during the repair of a UV-NIL mold. There are two methods for controlling static. One is electron shower irradiation during FIB (Fig. 7(a)). In this method, however, the region of electron irradiation is also deposited, as in FIB-CVD. This makes it very difficult to apply an electron shower as an antistatic method. The other method is using an antistatic agent spin-coated on the UV-NIL mold (Fig. 7(b)). In this case, the deposition by FIB irradiation is possible. We used a 20-nm thick ESPACER300Z (Showa Denko) as an antistatic agent to prevent electrical charge. The FIB-irradiated part on ESPACER300Z was first etched away and then the SiOx was deposited, as shown in Fig. 7(b). ESPACER300Z can easily be washed away with water after the repair.

We evaluated the antistatic effect of ESPACER300Z on a quartz substrate. We performed FIB-CVD using tetraethoxysilane on quartz substrates both with and without an antistatic agent. Figure 8 (a) and (b) shows the scanning ion microscopy (SIM) images of the 200-nm wide patterns fabricated by FIB-CVD at 1 pA on the two substrates. The line pattern was not formed on the substrate with no antistatic agent because of substrate drift caused by electrical charge. In contrast, the line pattern was clearly formed on the substrate that did use the antistatic agent, as shown in Fig. 8(b). Next, we fabricated 3D structures by FIB-CVD on ESPACER300Z-coated quartz substrates at 1 pA and 7 pA to examine the beam current dependency. When the beam current was 1 pA, the 3D structure was successfully fabricated on the quartz substrate, as shown in Fig. 9(a). However, as shown in Fig. 9(b), thorns were formed on the edges of the 3D structure fabricated by FIB-CVD at 7 pA.

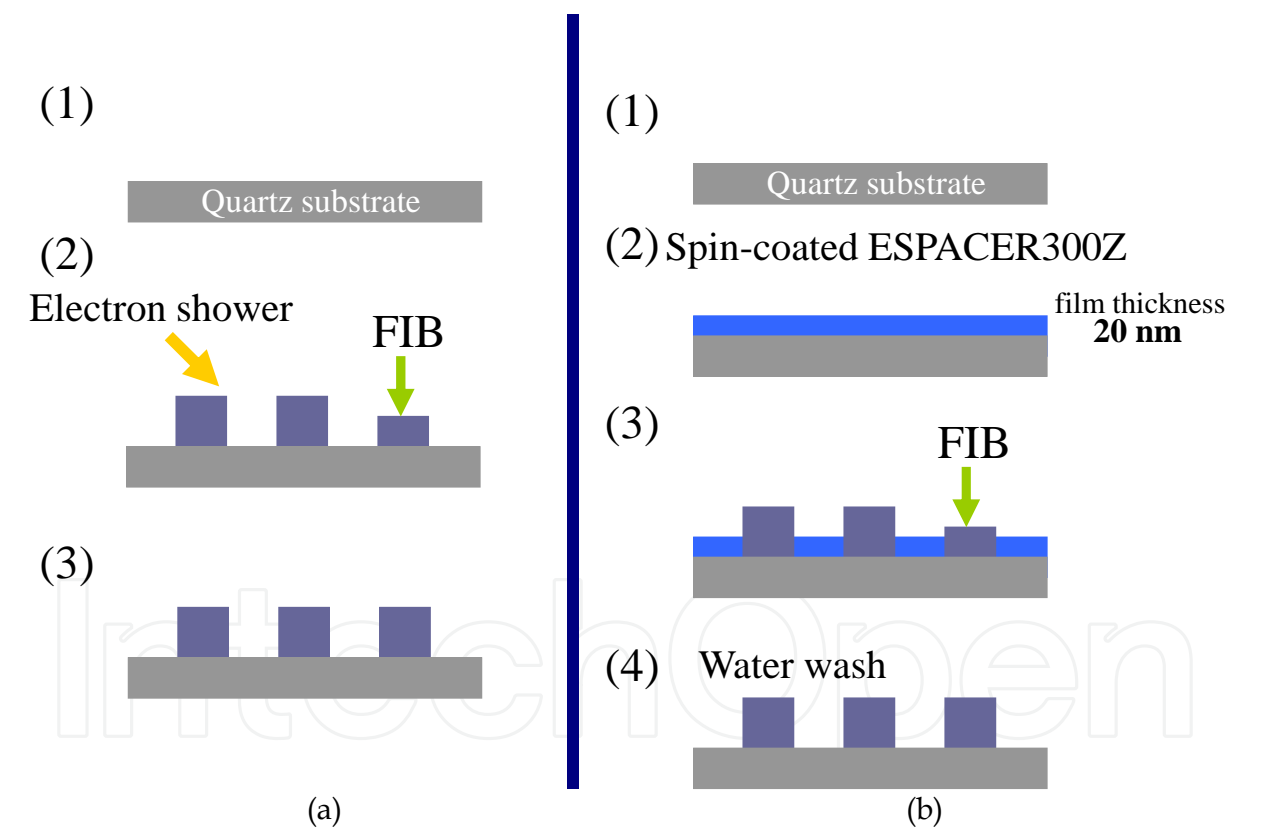


Fig. 7. Schematic of methods to control static: (a) FIB-CVD performed with an electron shower and (b) using an antistatic agent (ESPACER 300Z: Showa Denko Co.) spin-coated on the UV-NIL mold.

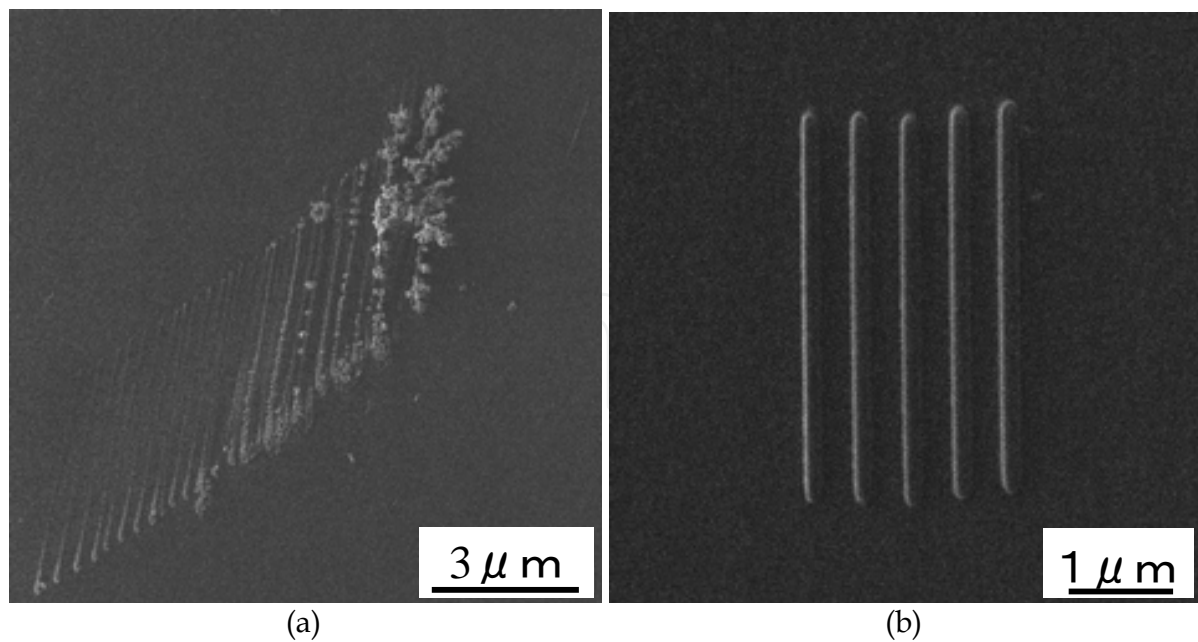


Fig. 8. SIM images of 200-nm wide patterns fabricated by FIB-CVD at 1 pA on quartz substrates without and with antistatic agent.

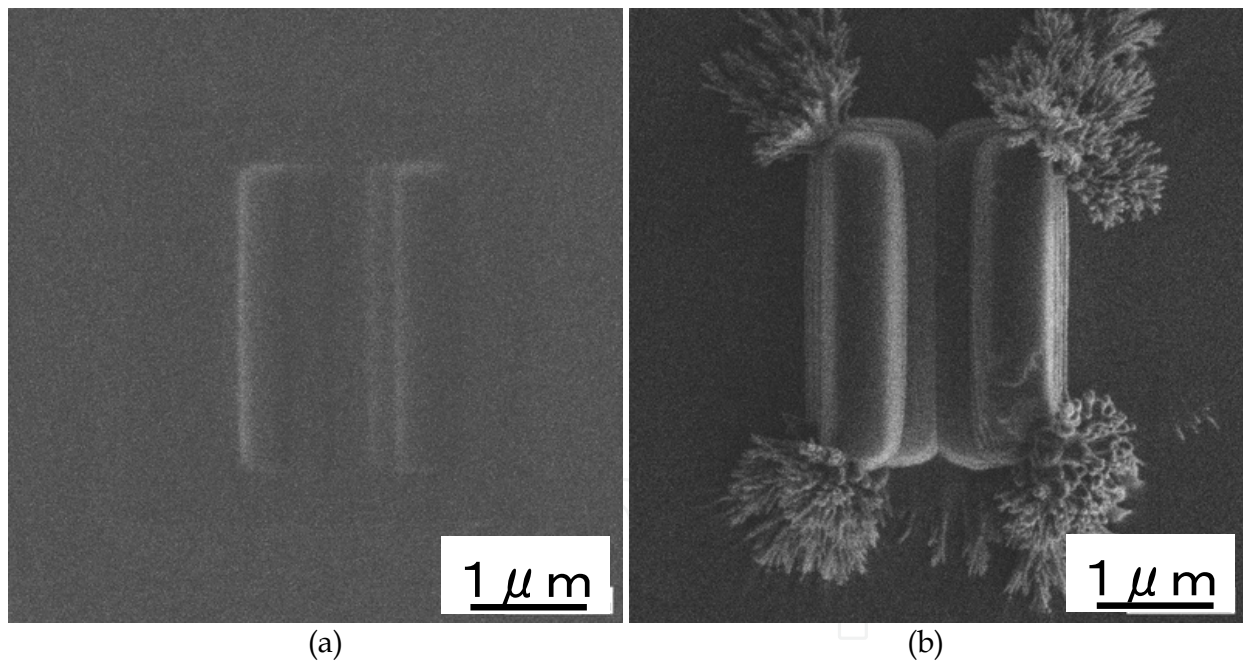


Fig. 9. (a) 3D structure fabricated by FIB-CVD with ESPACER300Z at 1 pA. (b) Thorns were formed on the corners of the 3D structure with ESPACER300Z at 7 pA.

To determine why the thorns were fabricated on the edges, we observed them by scanning transmission electron microscopy (STEM) and measured their atomic composition by SEM-EDX. Figure 10 shows the STEM images of the Au-coated thorns. Although the pillar fabricated by FIB-CVD has a gallium core due to Ga ion implantation, no such gallium core was observed in the thorns. According to the SEM-EDX results, the atomic composition of the thorns was 16% Si, 68% O, 13% C, and 3% Ga. In contrast, the atomic composition of the



3D structure was 21% Si, 51% O, 9% C, and 19% Ga. Ga content in the thorns was much less than that in the deposited SiO<sub>x</sub>. These results indicate that the thorn structure was caused by electric charge accumulation on the FIB-deposited region due to the increasing beam current. This makes it clear that we must use an optimum beam current to achieve hollow defect repair by FIB-CVD.

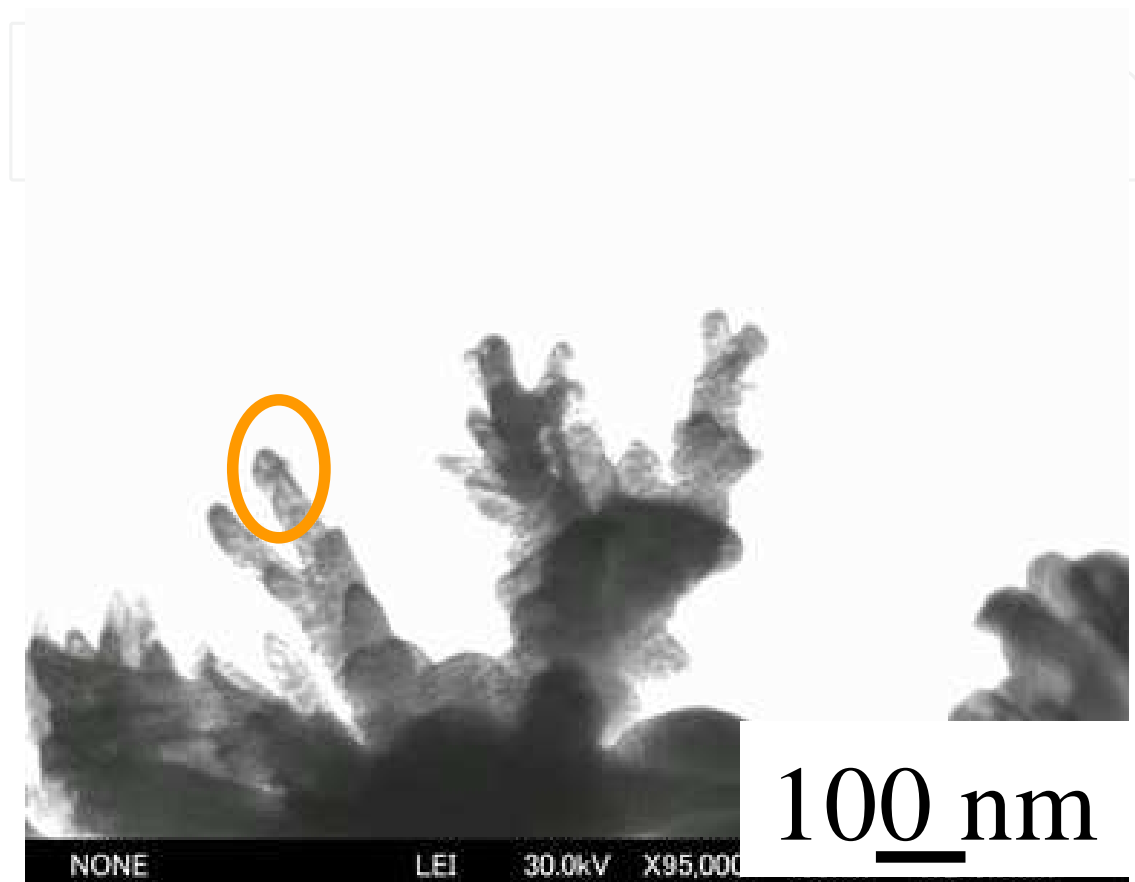


Fig. 10. STEM image of Au-coated thorns on 3D structure. The atomic content inside the circle was measured by SEM-EDX.

### 3.3 UV nanoimprint mold repair by FIB etching and CVD

To examine the repair resolution of the FIB etching, we fabricated a narrow line by FIB etching on a quartz mold and performed UV-NIL using this mold. The mold was pressed onto UV-curable resin (Toyo Gosei: PAK-01). The UV-NIL pressure and UV wavelength were 0.9 MPa and 365 nm, respectively. The mold was held for 90 sec during imprinting. The release agent (Daikin Industries; OPTOOL DSX: demnamsolvent = 1 : 1000 by weight) was precoated on the mold to avoid the adhesion of resin and to enable a smooth separation of the mold and the substrate. Figure 11(a) shows the imprinted line pattern using the mold on the PAK-01. The linewidth was 29 nm. Results demonstrated that FIB can etch a narrow line on the quartz substrate.

We also examined the repair resolution of FIB-CVD. First, we fabricated a narrow line by FIB etching, and then deposited it on the quartz mold by FIB-CVD. The pattern imprinted by UV-NIL using this mold is shown in Fig. 11(b). The fabricated narrow linewidth was 36 nm. These results indicate that a 30-nm defect can be repaired by FIB etching and CVD.

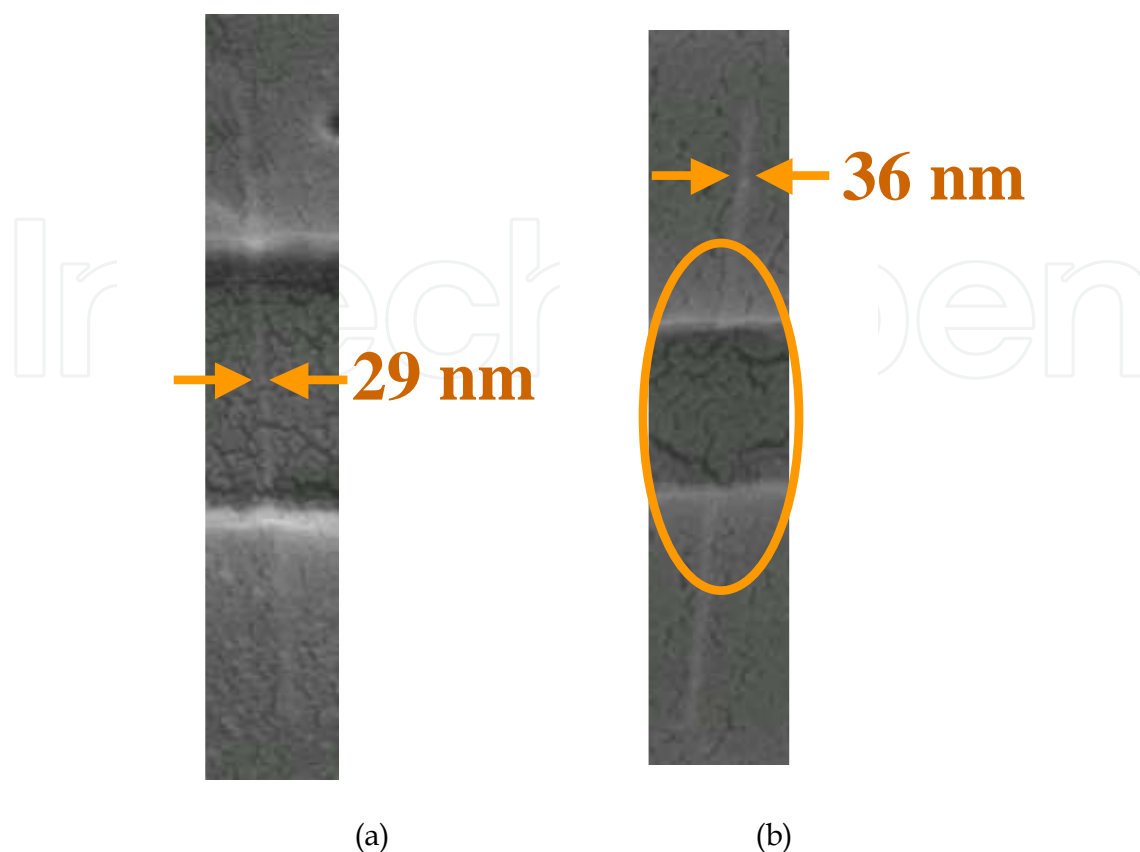


Fig. 11. SEM images of lines imprinted by UV-NIL using (a) quartz mold with narrow hollow-line fabricated by FIB etching and (b) repaired mold.

### 3.3.1 Repair of protrusion defects on UV-NIL mold

To repair a UV-NIL mold by 30-kV FIB etching at 1 pA, we fabricated program protrusion defects on it using a quartz substrate by EB lithography and RIE. Figure 12(a) shows the program protrusion-defective template. The protrusion width and length were 40 nm and 150 nm, respectively. Figure 12(b) shows the defective line pattern transferred by UV-NIL on the PAK-01 and as we can see, the defective line pattern was clearly imprinted on the substrate. We repaired the protrusion defects on the UV-NIL mold by FIB etching. Figure 13(a) shows the line pattern repaired by FIB etching on the mold. The repair time for one protrusion defect was about 10 sec. The protrusion defect was successfully etched away by FIB and the repaired line pattern was clearly imprinted (Fig. 13(b)).

### 3.3.2 Repair of hollow defects on UV-NIL mold

Figure 14(a) shows the program hollow-defective mold. The hollow-width was 60 nm. Figure 14(b) shows the imprinted line pattern using the defective mold on the substrate. The defective line pattern was clearly imprinted on the substrate. We repaired the hollow defect on the UV-NIL mold by FIB-CVD. Figure 15(a) shows the line pattern on the mold repaired by FIB-CVD using tetraethoxysilane. The repair time for one hollow defect was about 20 sec. Figure 15(b) shows the line pattern transferred using the repaired mold on the substrate. The hollow defect region was successfully deposited by FIB-CVD, and the repaired line pattern was clearly imprinted (Fig. 15(b)).

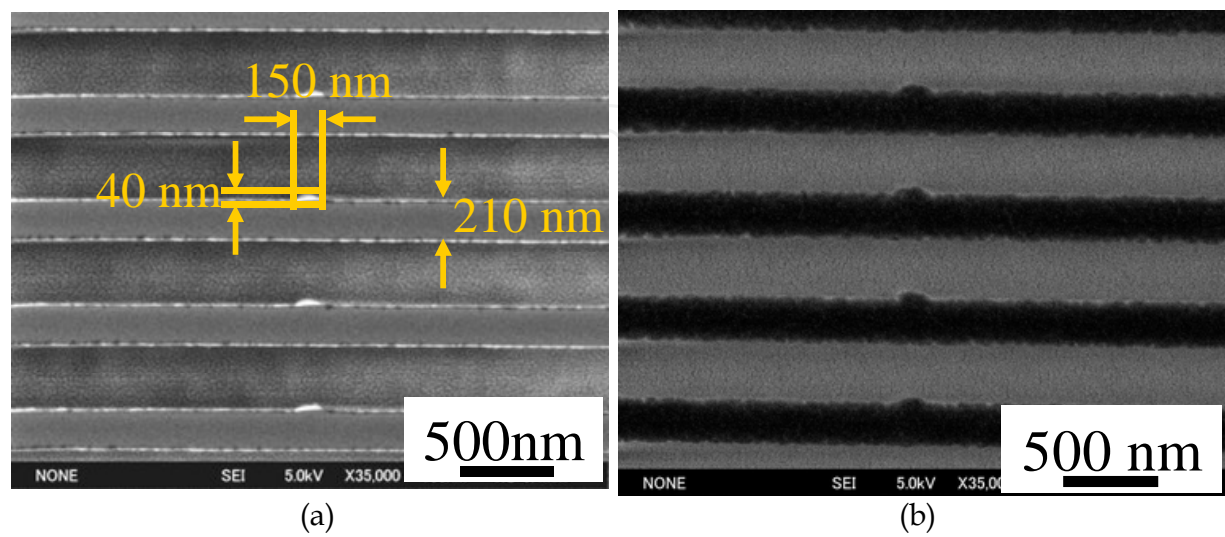


Fig. 12. SEM images of (a) program protrusion-defective quartz mold and (b) PAK-01 defective line pattern imprinted by UV-NIL using the protrusion-defective quartz mold.

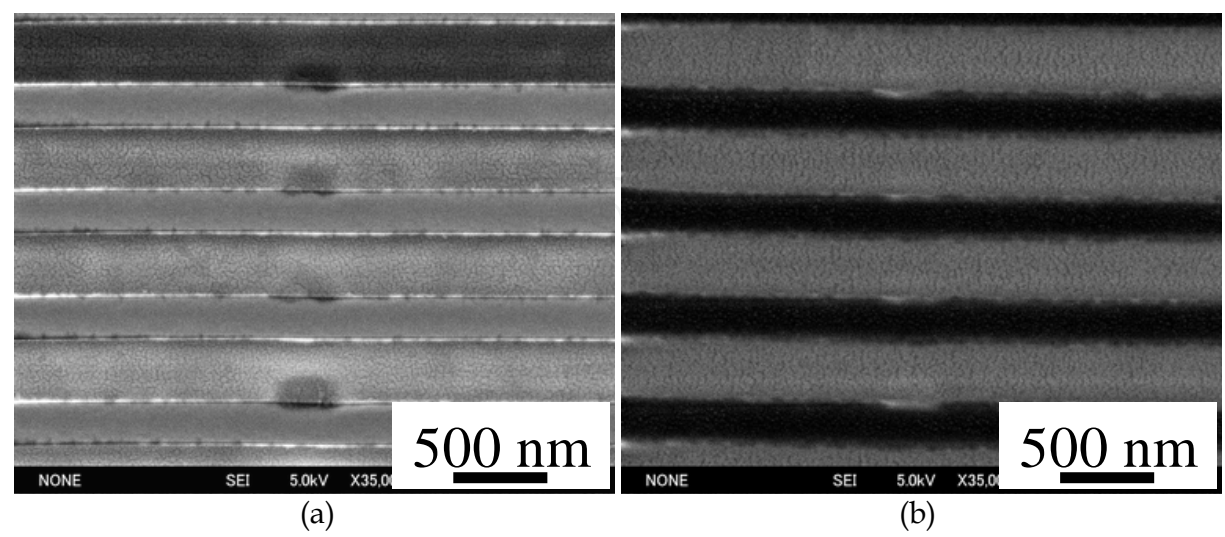


Fig. 13. SEM images of (a) line pattern in Fig. 12(a) repaired by FIB etching and (b) PAK-01 line pattern imprinted by UV-NIL using the repaired quartz mold.

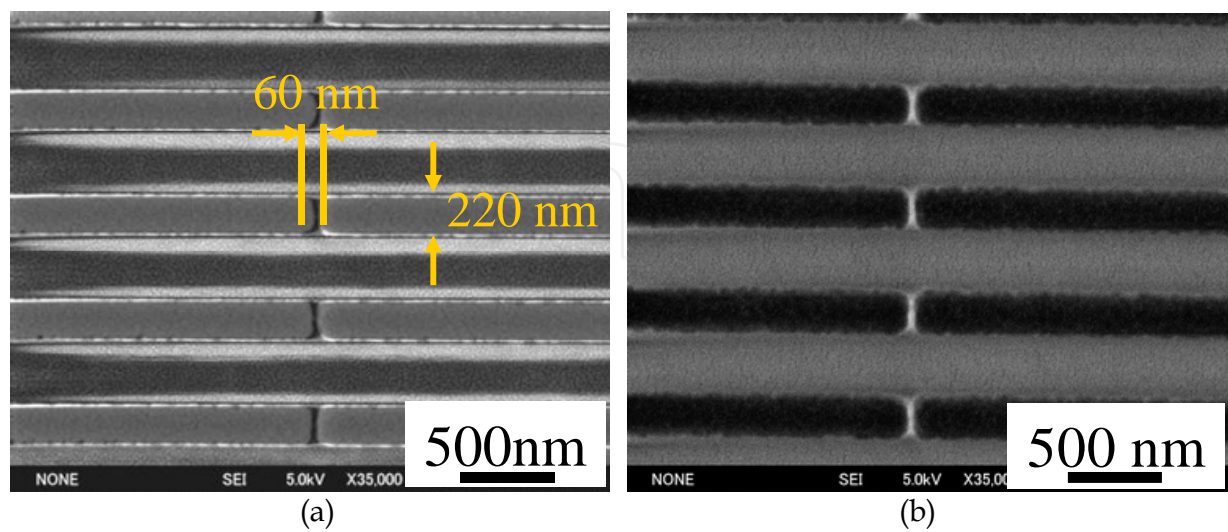


Fig. 14. SEM images of (a) program hollow defective quartz mold and (b) PAK-01 defective line pattern imprinted by UV-NIL using the hollow defective quartz mold.

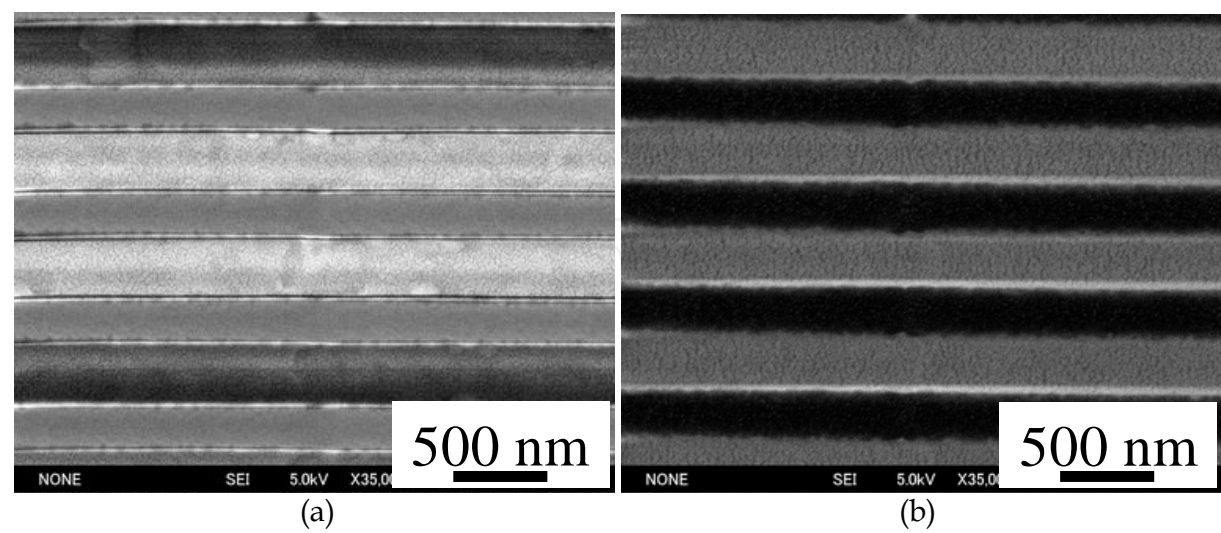


Fig. 15. SEM images of (a) line pattern repaired by FIB-CVD on quartz mold and (b) PAK-01 line pattern imprinted by UV-NIL using the repaired quartz mold.



The durability of a repaired mold is crucial for applying UV-NIL to mass production. Therefore, we tested the durability of the SiO<sub>x</sub> material deposited by FIB-CVD by observing over 200 repeated uses of the mold repaired by FIB-CVD. Figure 16(a) and (b) shows the SEM images of the 100th and 200th imprinted pattern. After nanoimprintings, the pattern was still clearly imprinted on the resin. This result indicates that the deposited SiO<sub>x</sub> material has sufficient durability for repeated UV-NIL.

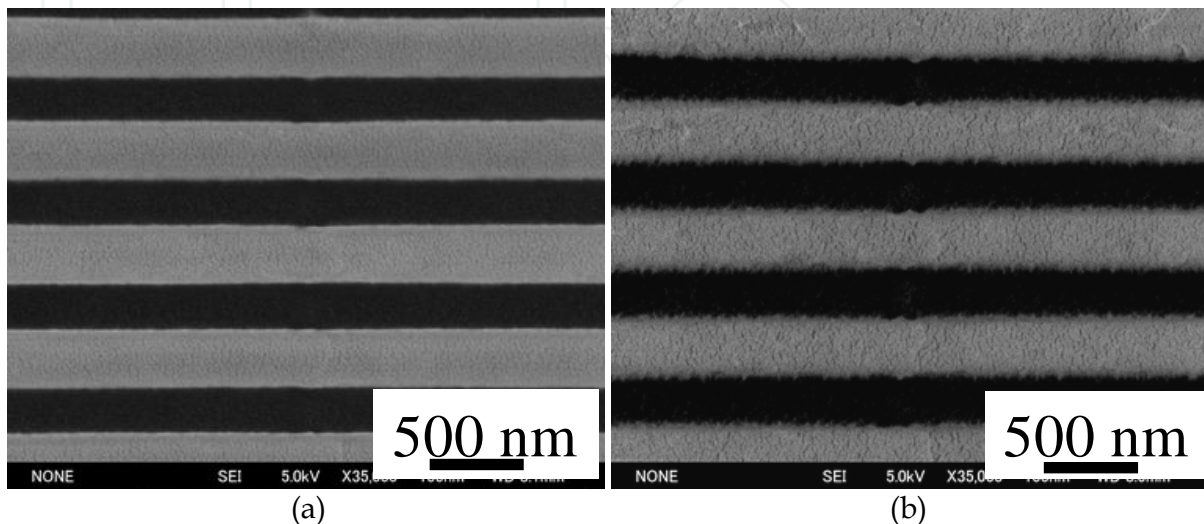


Fig. 16. SEM images of (a) 100th and (b) 200th imprinted patterns on PAK-01 formed by UV-NIL using quartz mold repaired by FIB-CVD.

#### 4. Conclusion

We repaired NIL molds by FIB etching and CVD. In the case of a T-NIL mold, we used phenanthrene as a source gas to repair the hollow-defect by FIB-CVD. The deposited material was DLC containing gallium. However, the gallium evaporation from DLC did not occur during T-NIL because gallium's evaporation temperature is about 500 °C. The protrusion- and hollow-defective SiO<sub>2</sub>/Si molds were successfully repaired by FIB etching and CVD and the lines were clearly imprinted by T-NIL using the repaired mold.

In UV-NIL, UV-curable resin is irradiated by UV through a UV-NIL mold. This means that phenanthrene cannot be used as a source gas in FIB-CVD because the deposited DLC is not transparent. We therefore used SiO<sub>x</sub> material deposited by FIB-CVD using tetraethoxysilane as the source gas. We measured the transmittance and hardness of the SiO<sub>x</sub> film deposited by FIB-CVD, and results demonstrated that the deposited SiO<sub>x</sub> material has sufficient transmittance and hardness to perform UV-NIL.

To repair the defective UV-NIL mold, we must consider the effect of electrical charge because the material of UV-NIL molds is usually quartz. We proposed the use of an antistatic agent to prevent electrical charge because the antistatic agent can be spin-coated on the UV-NIL mold and is easy to wash away with water after the repair. However, failure to use an optimum beam current in FIB-CVD resulted in the fabrication of thorns. This highlights the need for an optimum beam current if we want to achieve hollow defect repair by FIB-CVD.

We repaired the defective quartz mold by FIB etching and CVD and performed UV-NIL using the repaired mold. The repaired lines were clearly imprinted on the resin. Results demonstrated that the deposited SiO<sub>x</sub> material has a sufficient durability for repeated UV-NIL.

In this work, we used gallium-FIB to repair the NIL molds. Recently, helium ion microscopy (HIM) with a subnanometer probe size has become commercially available. Apart from the obvious advantage of small probe sizes, HIM also boasts a narrow interaction volume in the substrate and the predominance of secondary electron emission. A helium ion microscope can also be used for nanofabrication. We expect the mold repair resolution to dramatically improve by using HIM.

## 5. References

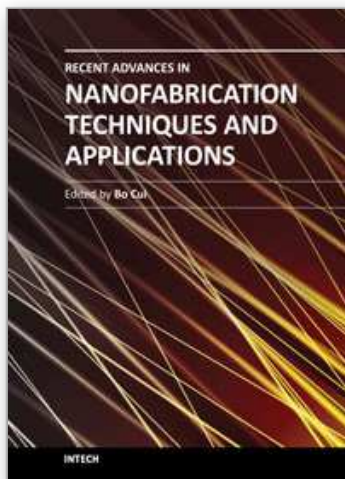
- Chou, S. Y.; Krauss, P. R. & Renstrom, P. J. (1995). Imprint of sub-25 nm vias and trenches in polymers. *Applied Physics Letter*, Vol.67, No.21, (September 1995), pp. 3114-3116, ISSN 003-6951
- Chou, S. Y.; Krauss, P. R. & Renstrom, P. J. (1996). Imprint Lithography with 25-Nanometer Resolution. *Science*, Vol.272, No.5258, (April 1996), pp. 85-87, ISSN 0036-8075
- Chou, S. Y.; Krauss, P. R.; Zhang, W.; Guo, L. & Zhuang, L. (1997). Sub-10 nm imprint lithography and applications. *Journal of Vacuum Science & Technology B*, Vol.15, No.6, (September 1997). pp. 2897-2904, ISSN 0734-211X
- Fuchs, A.; Bender, M.; Plaschotka, U. ; Kock, L.; Wahlbrink, T.; Gottlob, H.; Efavi, J.; Moeller, M.; Schmidt, M.; Mollenhauer, T.; Moormann, C.; Lemme, M. & Kurz, H. (2006). Nanowire fin field effect transistors via UV-based nanoimprint lithography, *Journal of Vacuum Science & Technology B*, Vol.24, No.6, (November 2006). pp. 2964-2967, ISSN 0734-211X
- Yoshitake, S.; Sunaoshi, H.; Yasui, K.; Kobayashi, H.; Sato, T.; Nagarekawa, O.; Thompson, E.; Schmid, G. & Resnick, J. (2007), The development of full field high resolution imprint templates, *Photomask Technology 2007 (Proceedings Volume) Proceedings of SPIE*, pp.67300E, ISBN 9780819468871 6730, Monterey, California, USA, September,2007
- Schmid, G. M.; Stewart, M. D.; Wetzel, J.; Palmieri, F.; Hao, J.; Nishimura, Y.; Jen, K.; Kim, E. K.; Resnick, D. J., Liddle, J. A. & Willson, C. G. (2006), Implementation of an imprint damascene process for interconnect fabrication. *Journal of Vacuum Science & Technology B*, Vol.24, No.3, (May 2006). pp. 1283-1291, ISSN 0734-211X
- Ahn, S.W.; Lee, K. D.; Kim, J. S.; Kim, S. H.; Park, J. D.; Lee, S. H. & Yoon, P. W. (2005), Fabrication of a 50 nm half-pitch wire grid polarizer using nanoimprint lithography, *Nanotechnology*, Vol.16, No.9, (July 2005). pp.1874-1877, ISSN 0957-4484
- Wang, J. J.; Deng, X. G.; Liu, X. M.; Nikolov, A.; Sciortino, P.; Liu, F. & Chen, L. (2006), Ultraviolet wave plates based on monolithic integration of two fully filled and planarized nanograting layers, *Optics Letters*, Vol.31, No.12, (April 2006). pp.1893-1895, ISSN 0146-9592
- Beck, M.; Persson, F.; Carlber, P.; Graczyk, M.; Maximov, I.; Ling, T. G. I. & Montelius, L. (2004), Nanoelectrochemical transducers for (bio-) chemical sensor applications fabricated by nanoimprint lithography, *Microelectronic Engineering*, Vol.73-74, (June 2004). pp.837-842, ISSN 0167-9317
- Nomura, S.; Kojima, H.; Ohyabu, Y.; Kuwabara, K.; Miyauchi, A. & Uemura, T. (2005), Cell Culture on Nanopillar Sheet: Study of HeLa Cells on Nanopillar Sheet, *Japanese*

- Journal of Applied Physics*, Vol.44, No.37, (September 2005). pp.L1184-L1186, ISSN 0021-4922
- Kim, M. S.; Kim, J. S.; Cho, J. C.; Shtein, M.; Guo, L. J. & Kim, J. (2007), Flexible conjugated polymer photovoltaic cells with controlled heterojunctions fabricated using nanoimprint lithography, *Applied Physics Letter*, Vol.90, No.12, (March 2007), pp. 123113-1-123113-3, ISSN 003-6951
- Haisma, J.; Verheijen, M. & Heuvel, K. V. D. (1996), Mold-assisted nanolithography: A process for reliable pattern replication, *Journal of Vacuum Science & Technology B*, Vol.14, No.6, (August 1996). pp. 4124-4128, ISSN 0734-211X
- Bailey, T.; Choi, B. J.; Colburn, M.; Meissi, M.; Shaya, S.; Ekerdt, J. G.; Sreenivasan, S. V. & Willson, C. G. (2000), Step and flash imprint lithography: Template surface treatment and defect analysis, *Journal of Vacuum Science & Technology B*, Vol.18, No.6, (September 2000). pp. 3572-3577, ISSN 0734-211X
- Komuro, M.; Taniguchi, J.; Inoue, S.; Kimura, N.; Tokano, Y.; Hiroshima, H. & Matsui, S. (2000), Imprint Characteristics by Photo-Induced Solidification of Liquid Polymer, *Japanese Journal of Applied Physics*, Vol.39, No.12B, (October 2000). pp.7075-7079, ISSN 0021-4922
- Xia, Y. & Whitesides, G. M. (1998), Soft Lithography, *Annual Reviews Materials Research*, Vol.28, (August 1998). pp. 153-184, ISSN 1531-7331
- Libioulle, L.; Bietsch, A.; Schmid, H.; Michel, B & Delamarche, E. (1999), Contact-Inking Stamps for Microcontact Printing of Alkanethiols on Gold, *Langmuir*, Vol.15, No.2, (December 1999). pp. 300-304, ISSN 0743-7463
- Plachetka, U.; Bender, M.; Fuchs, A., Vratzov, B; Glinsner, T.; Lindner, F. & Kurz, H. (2004), Wafer scale patterning by soft UV-Nanoimprint Lithography, *Microelectronic Engineering*, Vol.73-74, (June 2004). pp.167-171, ISSN 0167-9317
- Matsui, S.; Igaku, Y.; Ishigaki, H.; Fujita, J.; Ishida, N.; Ochiai, Y.; Komuro, M. & Hiroshima, H. (2001), Room temperature replication in spin on glass by nanoimprint technology, *Journal of Vacuum Science & Technology B*, Vol.19, No.6, (September 2001). pp. 2801-2805, ISSN 0734-211X
- Matsui, S.; Igaku, Y.; Ishigaki, H.; Fujita, J.; Ishida, N.; Ochiai, Y.; Namatsu, H. & Komuro, M. (2003), Room-temperature nanoimprint and nanotransfer printing using hydrogen silsesquioxane, *Journal of Vacuum Science & Technology B*, Vol.21, No.2, (February 2003). pp. 688-692, ISSN 0734-211X
- Nakamatsu, K.; Watanabe, K.; Tone, K.; Katase, T.; Hattori, W.; Ochiai, Y.; Matsuo, T.; Sasago, M.; Namatsu, H.; Komuro, M. & Matsui, S. (2004), Bilayer Resist Method for Room-Temperature Nanoimprint Lithography, *Japanese Journal of Applied Physics*, Vol.43, No.6B, (June 2004). pp.4050-4053, ISSN 0021-4922
- Nakamatsu, K.; Watanabe, K.; Tone, K.; Namatsu, H. & Matsui, S. (2005), Nanoimprint and nanocontact technologies using hydrogen silsesquioxane, *Journal of Vacuum Science & Technology B*, Vol.23, No.2, (March 2005). pp. 507-512, ISSN 0734-211X
- Heard, P. J. & Prewett, P. D. (1990), Focused ion beam deposition of carbon for photomask repair, *Microelectronic Engineering*, Vol.11, No. 1-4 (April 1990). pp.421-425, ISSN 0167-9317

- Matsui, S.; Kaito, T.; Fujita, J.; Komuro, M.; Kanda, K. & Haruyama, Y. (2000), Three-dimensional nanostructure fabrication by focused-ion-beam chemical vapor deposition, *Journal of Vacuum Science & Technology B*, Vol.18, No.6, (August 2000). pp. 3181-3184, ISSN 0734-211X
- Watanabe, K.; Kanda, K.; Haruyama, Y.; Kaito, T. & Matsui, S. (2004), Nanoimprint Mold Repair by Ga<sup>+</sup> Focused-Ion-Beam Direct Etching, *Japanese Journal of Applied Physics*, Vol.43, No.11A, (November 2004). pp.7769-7772, ISSN 0021-4922
- Fujita, J.; Ishida, M.; Ichihashi, T.; Ochiai, Y.; Kaito, T & Matsui, S. (2003), Growth of three-dimensional nano-structures using FIB-CVD and its mechanical properties, *Nuclear Instruments and Methods in Physics Research Section B: Beam Interactions with Materials and Atoms*, Vol.206, No. (May 2003). pp. 472-477, ISSN 0168-583X
- Igaki, J.; Saikubo, A.; Kometani, R.; Kanda, K.; Suzuki, T.; Niihara, K. & Matsui, S. (2007), Elementary Analysis of Diamond-Like Carbon Film Formed by Focused-Ion-Beam Chemical Vapor Deposition, *Japanese Journal of Applied Physics*, Vol.46, No.12, (December 2007). pp.8003-8004, ISSN 0021-4922
- Kanda, K.; Igaki, J.; Saikubo, A.; Kometani, R.; Suzuki, T.; Niihara, K.; Saito, H & Matsui, S. (2008), Effects of Annealing on Material Characteristics of Diamond-Like Carbon Film Formed by Focused-Ion-Beam Chemical Vapor Deposition, *Japanese Journal of Applied Physics*, Vol.47, No.9, (September 2008). pp.7464-7466, ISSN 0021-4922
- Kanda, K.; Okada, M.; Kang, Y.; Niibe, M.; Wada, A.; Ito, H.; Suzuki, T. & Matsui, S. (2010), Structural Changes in Diamond-Like Carbon Films Fabricated by Ga Focused-Ion-Beam-Assisted Deposition Caused by Annealing, *Japanese Journal of Applied Physics*, Vol.49, (June 2010). pp.06GH06-1-06GH06-5, ISSN 0021-4922
- Edinger, K; Melingailis, J. & Orloff, J. (1998), Study of precursor gases for focused ion beam insulator deposition, *Journal of Vacuum Science & Technology B*, Vol.16, No.6, (September 1998). pp. 3311-3314, ISSN 0734-211X
- Okada, M.; Nakamatsu, K.; Kanda, K.; Haruyama, Y.; Kometani, R.; Kaito, T. & Matsui, S. (2008), Examination of Focused-Ion-Beam Repair Resolution for UV-Nanoimprint Templates, *Japanese Journal of Applied Physics*, Vol.47, Vol.6 (June 2008). pp.5160-5163, ISSN 0021-4922
- Campbell, A. N.; Peterson, K. A.; Fleetwood, D. M. & Soden, J. M. (1997), Effects of focused ion beam irradiation on MOS transistors, *Proceedings of International Reliability Physics Symposium*, pp.72-81, ISBN 0-7803-3575-9, Piscataway, New Jersey, USA, April, 1997
- Saida, Y.; Okubo, T.; Sasaki, J.; Konishi, T. & Morita, M. (2005), Evaluation of the new-type ESPACER adopted for its removal after post-exposure bake process, *Photomask and Next-Generation Lithography Mask Technology XII Proceedings of SPIE*, ISBN 0819449962, Yokohama, Kanagawa, Japan, April 2005
- Ward, B. W.; Notte, J. A. & Exonomou, N. P. (2006), Helium ion microscope: A new tool for nanoscale microscopy and metrology, *Journal of Vacuum Science & Technology B*, Vol.24, No.6, (November 2006). pp. 2871-2874, ISSN 0734-211X



- Alkemadea, P. F. A.; Chen, P.; Veldhoven, E. V. & Maas, M. (2010), Model for nanopillar growth by focused helium ion-beam-induced deposition, *Journal of Vacuum Science & Technology B*, Vol.28, No.6, (December 2010). pp. C6F22-C6F25, ISSN 0734-211X
- Livengood, R.; Tan, S.; Greenzweig, Y.; Notte, J. & McVey, S. (2009), Subsurface damage from helium ions as a function of dose, beam energy, and dose rate, *Journal of Vacuum Science & Technology B*, Vol.27, No.6, (December 2009). pp. 3244-3249, ISSN 0734-211X



## **Recent Advances in Nanofabrication Techniques and Applications**

Edited by Prof. Bo Cui

ISBN 978-953-307-602-7

Hard cover, 614 pages

**Publisher** InTech

**Published online** 02, December, 2011

**Published in print edition** December, 2011

Nanotechnology has experienced a rapid growth in the past decade, largely owing to the rapid advances in nanofabrication techniques employed to fabricate nano-devices. Nanofabrication can be divided into two categories: "bottom up" approach using chemical synthesis or self assembly, and "top down" approach using nanolithography, thin film deposition and etching techniques. Both topics are covered, though with a focus on the second category. This book contains twenty nine chapters and aims to provide the fundamentals and recent advances of nanofabrication techniques, as well as its device applications. Most chapters focus on in-depth studies of a particular research field, and are thus targeted for researchers, though some chapters focus on the basics of lithographic techniques accessible for upper year undergraduate students. Divided into five parts, this book covers electron beam, focused ion beam, nanoimprint, deep and extreme UV, X-ray, scanning probe, interference, two-photon, and nanosphere lithography.

### **How to reference**

In order to correctly reference this scholarly work, feel free to copy and paste the following:

Makoto Okada and Shinji Matsui (2011). Repairing Nanoimprint Mold Defects by Focused-Ion-Beam Etching and Deposition, Recent Advances in Nanofabrication Techniques and Applications, Prof. Bo Cui (Ed.), ISBN: 978-953-307-602-7, InTech, Available from: <http://www.intechopen.com/books/recent-advances-in-nanofabrication-techniques-and-applications/repairing-nanoimprint-mold-defects-by-focused-ion-beam-etching-and-deposition>

**INTECH**  
open science | open minds

### **InTech Europe**

University Campus STeP Ri  
Slavka Krautzeka 83/A  
51000 Rijeka, Croatia  
Phone: +385 (51) 770 447  
Fax: +385 (51) 686 166  
[www.intechopen.com](http://www.intechopen.com)

### **InTech China**

Unit 405, Office Block, Hotel Equatorial Shanghai  
No.65, Yan An Road (West), Shanghai, 200040, China  
中国上海市延安西路65号上海国际贵都大饭店办公楼405单元  
Phone: +86-21-62489820  
Fax: +86-21-62489821

© 2011 The Author(s). Licensee IntechOpen. This is an open access article distributed under the terms of the [Creative Commons Attribution 3.0 License](https://creativecommons.org/licenses/by/3.0/), which permits unrestricted use, distribution, and reproduction in any medium, provided the original work is properly cited.

IntechOpen

IntechOpen